SAINS TANAH – Journal of Soil Science and Agroclimatology

Journal homepage: http://jurnal.uns.ac.id/tanah

Soil hydraulic properties and field-scale hydrology as affected by land-management options

Atiqur Rahman*, M. G. Mostofa Amin

Department of Irrigation and Water Management, Bangladesh Agricultural University, Mymensingh 2202, Bangladesh

ARTICLE INFO

Keywords:
Bulk density
Hydrological functioning
HYDRUS-1D
Plow pan
Runoff

Article history
Submitted: 2023-01-16
Accepted: 2023-04-07
Available online: 2023-06-30
Published regularly: June 2023

* *Corresponding Author*
Email address:
atiqur.20250302@bau.edu.bd

ABSTRACT

Recurring puddling for long-term rice cultivation forms a plow pan at a particular soil depth, which alters soil hydraulic properties, field-scale hydrology, and nutrient persistence in the soil. This experiment aimed to assess the impact of long-term rice cultivation on root-zone soil hydraulic properties and field-scale hydrology. Soil core samples were collected from four land management options namely, rice–rice, non-rice, rice and non-rice, and field ridge, at two sites, one with loam and another with silt-loam soil. The soil cores were sampled for each 10 cm layer up to 100 cm depth from three locations of each rotation at both sites. Soil hydraulic parameters were estimated using a pedotransfer function based on the measured bulk density and soil texture. A mathematical model named HYDRUS-1D predicted infiltration, percolation, and surface runoff with the estimated hydraulic properties for three extreme rainfall events, i.e., 3.33, 5, and 6.66 cm hr^{-1}, during a 3-hour period. A plow pan was found at 20–30 cm soil depth for all the land management options but not for the field ridge. The plow pan of the rice–rice rotation had the highest bulk density (1.53 g cm^{-3}) and the lowest hydraulic conductivity (17.56 cm day^{-1}). However, the top 10 cm soil layer in the rice–rice field had the lowest bulk density (0.93 g cm^{-3}). At both sites, the field ridge had higher infiltration and percolation and lower runoff than other rotations. The study reveals that the field-ridge area of a rice field can be the main water loss pathway. Phosphorus concentration in the rice-rice rotation decreased from 7.7 mg kg^{-1} in the 10-cm soil layer to 2.49 mg kg^{-1} in the 100-cm layer. These findings will facilitate making better water management decisions.

How to Cite: Rahman, A., Amin, M.G.M. (2023). Soil hydraulic properties and field-scale hydrology as affected by land-management options. Sains Tanah Journal of Soil Science and Agroclimatology, 20(1): 124-139. https://dx.doi.org/10.20961/stjssa.v20i1.70504

1. INTRODUCTION

Rice is the staple crop in many Asian countries, and its global annual per-person consumption is over 50 kg (Carrijo et al., 2017). Moreover, rice demand is increasing in proportion to the ever-increasing population. Rice production increased by more than 50% between 2000 and 2018, which is approximately 0.8 billion tonnes (FAO, 2020). Rice is grown under several water management conditions, including irrigated, rainfed upland, rainfed lowland, and deep water or floating rice (Datta et al., 2017). Depending on the growing season, climatic conditions, soil type, and hydrological conditions (Chauhan et al., 2017), nearly 566 to 1360 mm of water is required in rice fields (Amin et al., 2021). Water input depends on local climate, soil characteristics, and hydrological conditions (Chauhan et al., 2017). Heavy-textured soils with shallow water tables may require as little as 400 mm of water, whereas coarse-textured soils with deep water tables may need up to 2000 mm of water (Cabangon et al., 2004). The water productivity ranges from 0.2 to 1.2 kg m^{-3}, and the water use efficiency is merely 36.4% due to water losses through percolation, seepage, and runoff (Pereira et al., 2012; Xu et al., 2019). Therefore, it is necessary to study rice field hydrology and major water loss pathways.

Puddling before rice transplanting is a common practice. Puddling can be defined as tillage practices in a water-saturated field condition. The process breaks soil aggregates and reshuffles the soil particles, particularly at the 10–30 cm soil depth, and generates minute soil particles that end up filling the pore spaces (Mondal et al., 2016). As a result, the macropores are sealed off when the particles are settled down (Islam et al., 2014). Moreover, the macropore volume decreases, which remarkably reduces the soil pore connectivity (Chen et al., 2014; Islam et al., 2021) and hydraulic conductivity (Talukolaee et al., 2018). An illuviation process—accumulation of dissolved or suspended soil materials in one area or layer as a result of percolation from another—occurs between puddled topsoil and non-puddled subsoil that helps develop a plow pan with the lowest hydraulic conductivity (Shao et al., 2017). Therefore, the soil profile in rice fields is horizontally layered due to plowing and puddling effects consisting of three soil layers, namely, a saturated muddy layer with lower density and higher hydraulic conductivity, a plow pan layer, and non-puddled sub-soil (Mairghany et al., 2019; Xu et al., 2019). The plow pan impedes vertical water movement, which helps the non-puddled subsoil remain unsaturated (Patil & Das, 2013; Shao et al., 2017).

Rice field hydrology has three important influencing features, namely, the plow pan, the field ridge, and cracks that facilitate preferential flow (Neumann et al., 2009). Cracks are formed in the rice fields due to alternate wetting and drying irrigation but not for continuous flood irrigation. Soil hydraulic conductivity is 2.5–4.5 times higher in cracked paddy fields than in paddy fields without cracks. Cracks act as a preferential flow pathway, but a plow pan significantly reduces the preferential flow because most of the cracks are not able to penetrate the plow pan (Yi et al., 2020; Zhang et al., 2016; Zhang et al., 2014). However, the field ridge remains intact during the tillage operations. As a result, the plow pan may not develop beneath the field ridge, which may affect the water loss from the rice fields (He et al., 2017; Zhang et al., 2014).

Altered soil hydraulic properties may affect the transport of nutrients and contaminants (Amin et al., 2016). Dislodged colloids during puddling can remarkably influence the transportation of sorbing pollutants in the vadose zone. For instance, immobile colloids can adsorb pollutants and be deposited in micropores. As a result, the pollutants cannot move readily through the subsoil (Zhang, 2008). However, mobile colloids that adsorb pollutants can move easily through the macropores of the subsoil (Fang et al., 2016; Tang et al., 2020). These movement processes are true for phosphorus because it is likely to bind with colloids, particularly to iron oxides (Zhang, 2008).

The movement of water in paddy fields is a complex process, and it is time-consuming to measure infiltration, runoff, and percolation under field conditions. Therefore, an increasing number of researchers use computer-based mathematical models to understand these complex processes. The HYDRUS-1D (Šimůnek et al., 2008) is such a model that is widely used for simulating water transport in vadose zone soil under different irrigation management practices (Kirkham et al., 2019; Li et al., 2014; Phogat et al., 2017). Therefore, besides the field experiment, we used the HYDRUS-1D model to predict infiltration, percolation, and surface runoff for different rainfall intensities under different soil conditions. We hypothesized that the different land-management options under different crop rotations would affect the soil hydraulic properties, and the maximum amount of water may be lost near the field ridges of irrigated fields. The findings of the study can help manage both soil and water more efficiently to reduce yield gaps of different crops. The study was conducted with the following objectives: (i) to quantify the impact of long-term rice-rice rotation on soil hydraulic properties in the root zone compared to other crop rotations and; (ii) to investigate the effect of altered soil hydraulic properties on field-scale hydrology (infiltration, runoff, percolation) using the HYDRUS -1D model.

2. MATERIAL AND METHODS

2.1. Study site

This study was undertaken at two sites, i.e., the Bangladesh Agricultural University farm area (loam soil) and the Sutiakhali cropland area (silt loam soil), Mymensingh, Bangladesh. The study sites are located at 20°44´N and 90°25´E in the Old Brahmaputra Floodplain Agro-ecological Zone (Fig. 1). The proportions of sand, silt, and clay were 40%, 50%, and 10% in the loam soil and 27%, 68%, and 5% in the silt loam soil, respectively. The climatic condition of the study area is subtropical, with an average annual rainfall of 368 cm and an average temperature of 25°C during 2008–2019.

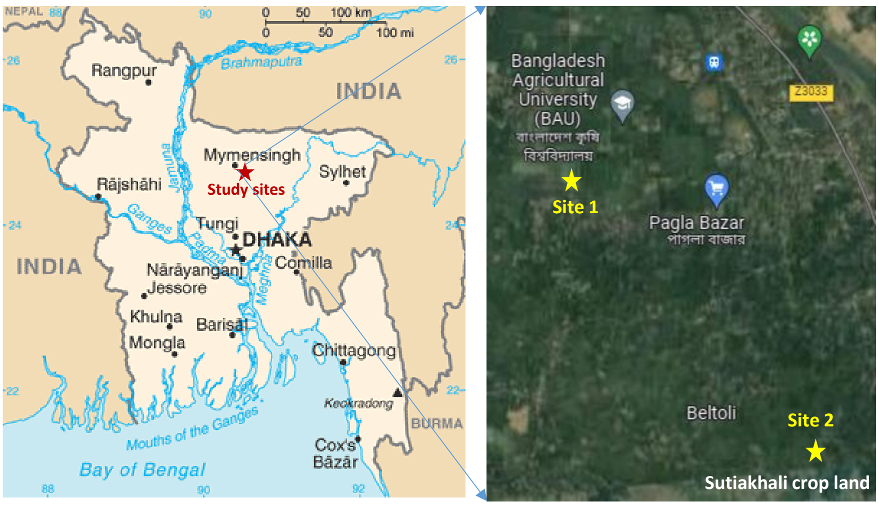

Figure 1. Experimental site location (Source: https://www.worldometers.info/maps/bangladesh-political-map/ and https://www.google.com/maps/@24.715789,90.4471511,13z

The reference evapotranspiration rate is lower in winter (2.9 mm day^{-1}), higher in dry summer (5.3 mm day^{-1}), and medium in the wet season (4.1 mm day^{-1}) (Ali et al., 2005). In the study area, the minimum depth to groundwater level was found in October and the maximum depth to groundwater level was found in April. The minimum depth to groundwater level in the deep and shallow aquifers was 7.5 and 4.4 m from the ground surface, respectively, whereas the maximum depth to groundwater level in the deep and shallow aquifers was found 12.8 and 6.2 m, respectively. Rice, maize, wheat, and vegetables are major crops in this area. Dry-season crops are mainly irrigated and wet-season crops are rainfed. Rice is grown both in wet and dry seasons. Fields are cultivated using tractors with a depth of 10–15 cm, and the rice fields are fertilized with chemical fertilizers, including inorganic nitrogen (N) (120 kg ha^{-1}) and phosphorus (P) (52.5 kg ha^{-1}).

2.2. Soil sampling

Soil core samplers (6.9 cm diameter and 8.75 cm height) were used to collect intact samples from different land-management options, namely, rice–rice which has been practiced since 2000, non-rice (mustard-wheat since 2010), mixed crop (rice-maize since 2014), rice-bare (since 2016), and field ridge. The field ridge was included as a land management option for two reasons. The first one was to compare the impacts of puddling operation in the rice field with the non-puddled field ridge soil, and the second one was to find out the potential water loss pathway in irrigated rice fields. In the rice-bare land management option, the land was planted with rice in the previous years, but the land was kept fallow for the last 4 years. The samples were collected in December 2020 after the harvesting of wet-season rice. The soil cores were sampled for each 10-cm layer up to 100-cm depth from three locations of each land management option at both sites. A total of 240 soil core samples were collected and analyzed in this study.

2.3. Weather data

Weather data, including maximum and minimum temperature, rainfall, wind speed, relative humidity, and sunshine hours, for the study period of 2020 were collected from the weather station located on the Bangladesh Agricultural University campus.

2.4. Estimation of soil hydraulic properties

The soil hydraulic parameters, namely saturated water content, residual water content, and saturated hydraulic conductivity (K_s), of the sampling layers were estimated by using a pedotransfer function called the RETC (RETention Curve) parameter optimization program (van Genuchten et al., 1991) based on the measured bulk density and soil texture. Pedotransfer functions work as a predictive tool to determine soil hydraulic properties based on soil parameters, such as soil texture and bulk density. The RETC pedotransfer function is a built-in tool of the HYDRUS-1D model (Šimůnek et al., 2009). The soil hydraulic properties of one location were also estimated by the inverse modeling technique and manual calibration technique using the HYDRUS-1D model against a set of measured soil water content data. The soil hydraulic properties estimated by the pedotransfer function and by the HYDRUS-1D model were compared to assess the accuracy of the pedotransfer function for this location.

2.5. Model description

The HYDRUS-1D model (Šimůnek et al., 2009) is used to simulate water, heat, and solute transport in variably saturated porous media. The model is widely used to calculate soil hydraulic properties by inverse modeling techniques and to predict soil water dynamics and irrigation requirements (Amin et al., 2014; Mo'allim et al., 2018; Vereecken et al., 2016). The governing equation of water movement through the soil medium is the one-dimensional Richards' equation, which is given below:

$$\frac{\partial \theta}{\partial t} = \frac{\partial}{\partial z}\left[K(\theta)\frac{\partial h}{\partial z} + K(\theta)\right] - S \quad ....[1]$$

where θ indicates the volumetric soil moisture content (cm^3 cm^{-3}), h represents the pressure head (cm), K is the unsaturated hydraulic conductivity (cm day^{-1}), z is associated with the depth below the soil surface (cm), t is the time (day), and S is the root water uptake (cm^3 cm^{-3} day^{-1}).

2.6. Model calibration and validation

The HYDRUS-1D model was calibrated and validated against different sets of measured soil water contents during two different 15-day long wetting-drying cycles. The initial conditions of the model were specified using the measured water contents. The soil surface was exposed to atmospheric boundary conditions. In this experiment, upper and lower boundary conditions were set as atmospheric boundary conditions with surface runoff and free drainage, respectively.

For the numerical domain of the geometry, a 100 cm soil profile depth was considered with ten different soil materials for the single-layer mass balance. The numerical domain consists of 101 nodes. The model was run for 72 hours with a maximum time step of one hour. We used the van Genuchten relationships (van Genuchten, 1980) to model the soil hydraulic properties, and no hysteresis was considered.

2.7. Estimation of field-scale hydrology

The soil hydraulic properties estimated by the pedotransfer function were used in the validated HYDRUS-1D model to estimate infiltration, percolation, and surface runoff for each crop rotation for three extreme rainfall events, i.e., 3.33 cm h^{-1}, 5 cm h^{-1}, and 6.66 cm h^{-1} of a 3 h duration.

2.8. Sample and data analysis

The physicochemical properties of the soil were analyzed using standard methods, such as soil textural class by a hydrometer, gravimetric soil water content by oven drying (105°C for 24 h), organic carbon by wet oxidation, and bulk density by determining the dry mass per unit volume of a given soil sample (McCarty et al., 2016). The persistence of P in different soil layers of the rice–rice rotation was determined. The available P concentration in the soil was determined by following Olsen's method (Watanabe & Olsen, 1965). All the required data were statistically analyzed by one-way Analysis of Variance using R software. The differences between the treatment means were tested with the Least Significant Difference (LSD) value at a statistical significance level of 0.05.

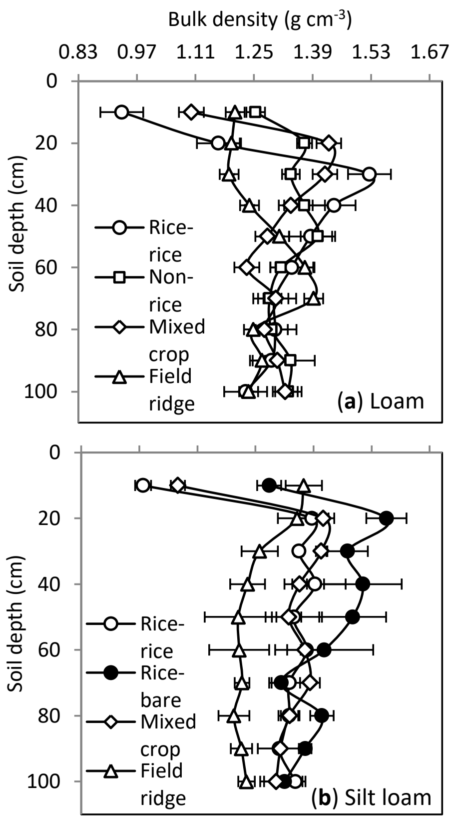

Figure 2. Bulk density at different soil depths for different crop rotations in (a) loam and (b) silt loam soil

3. RESULTS

3.1. Effects on soil properties

Increased bulk densities either in the 20 cm or 30 cm soil layer were observed for all crop rotations at both sites but not under the field ridge (Fig. 2). The results indicate that the traditional tillage operations in the crop fields formed a plow pan. In loam soil, the rice–rice rotation had a very pronounced plow pan compared to the other rotations. For the rice–rice rotation, the highest bulk density was 1.53 g cm^{-3} in the 30-cm soil layer (p = 0.001), followed by a gradual decrease and ended up with the value of 1.23 g cm^{-3} at the 100-cm soil layer. Kar et al. (2023a) conducted a study in the north-western Indian Himalayas with four treatments, namely control, conventional tillage, zero tillage, and reduced tillage, and quantified that bulk density in the conventional tillage system was higher among the treatments. Chen and Liu (2002) conducted a study in rice fields containing silt loam soil in Taiwan and found that the bulk density for 20–30 cm soil depth was 1.51 g cm^{-3}. The non-rice and mixed crop fields had a maximum bulk density between the 20-cm and 30-cm soil layers, with values of 1.37 (p = 0.009) and 1.43 g cm^{-3} (p = 0.001), respectively (Fig. 2a). Below the 60-cm soil layer, the crop rotations had no considerable impact on the bulk density (Table 1 and 2).

In silt loam soil, the rice-bare rotation has a long record of rice cultivation but has been kept as barren land for the last four years. This rotation had the highest bulk density of 1.57 g cm^{-3} in the 20-cm soil layer (p = 0.025). The rice-bare rotation had a relatively higher bulk density in the topsoil than the rice–rice rotation. The bulk density values of the rice–rice and mixed crop rotations followed almost the same pattern with depth. These two rotations had almost constant bulk densities below the 40-cm depth. The soil under the field ridge had the maximum bulk density (1.37 g cm^{-3}) in the top 10-cm soil layer (p = 0.00006) and had a value of 1.26 g cm^{-3} in the 30-cm layer before it almost leveled off with depth (Fig. 2 and Table 2).

Except for the field ridge, all the rotations had the lowest bulk density in the top 10-cm soil layer. For both soil textures, the rice–rice rotation had a very low bulk density in the top 10-cm layer, which can be attributed to the long-term puddling effect. Amin et al. (2014) experimented in a wheat field containing silty clay loam at the University of Agriculture Peshawar research farm and found that the bulk densities for the 0–20 cm and 20–40 cm soil layers were 1.49 g cm^{-3} and 1.54 g cm^{-3}, respectively, under moldboard tillage practice.

3.2. Effects on phosphorous persistence

To assess the effects of long-term rice cultivation on the soil persistence of P, the concentration of P in different soil layers up to 100-cm depth was measured. The highest P concentration was found in the top 10-cm soil layer (7.70 mg kg^{-1}), and the lowest concentration was found in the 100-cm soil layer (2.49 mg kg^{-1}).

Table 1. Measured bulk density values of loam soil at the Bangladesh Agricultural University farm area

Depth cm	Rice-rice (g/cc)	Non-rice (g/cc)	Mixed crop (g/cc)	Field ridge (g/cc)	LSD	P value	Significance level
10	0.93^{b}	1.25^{a}	1.10^{ab}	1.21^{a}	0.166	0.013	*
20	1.16^{b}	1.37^{a}	1.43^{a}	1.20^{b}	0.147	0.009	**
30	1.53^{a}	1.34^{b}	1.42^{b}	1.19^{c}	0.1	0.001	**
40	1.44^{a}	1.37^{a}	1.34^{a}	1.24^{a}	0.215	0.2	-
50	1.39^{a}	1.40^{a}	1.28^{a}	1.31a	0.143	0.222	-
60	1.34^{a}	1.31^{a}	1.23^{b}	1.37^{a}	0.05	0.005	**
70	1.30^{b}	1.29^{b}	1.30^{b}	1.39^{a}	0.072	0.039	*
80	1.30^{a}	1.29^{a}	1.28^{a}	1.25^{a}	0.084	0.501	-
90	1.29^{a}	1.34^{a}	1.31^{a}	1.27^{a}	0.109	0.527	-
100	1.23^{a}	1.33^{a}	1.32^{a}	1.24^{a}	0.144	0.318	-

Table 2. Measured bulk density values of silt loam soil at the Sutiakhali cropland area

Depth cm	Rice-rice (g/cc)	Non-rice (g/cc)	Mixed crop (g/cc)	Field ridge (g/cc)	LSD	P value	Significance level
10	0.98[d]	1.28[b]	1.06[c]	1.37[a]	0.08	0.00006	***
20	1.39[b]	1.57[a]	1.41[b]	1.35[b]	0.128	0.025	*
30	1.35[bc]	1.47[a]	1.41[ab]	1.26[c]	0.115	0.02	*
40	1.39[ab]	1.51[a]	1.36[ab]	1.23[b]	0.217	0.098	-
50	1.34[ab]	1.48[a]	1.33[ab]	1.21[b]	0.264	0.191	-
60	1.37[a]	1.42[a]	1.37[a]	1.21[a]	0.276	0.365	-
70	1.33[ab]	1.31[ab]	1.38[a]	1.22[b]	0.115	0.062	-
80	1.33[a]	1.41[a]	1.33[a]	1.20[b]	0.113	0.02	*
90	1.31[ab]	1.37[a]	1.31[ab]	1.22[b]	0.102	0.052	-
100	1.35[a]	1.32[a]	1.30[a]	1.23[a]	0.144	0.318	-

Table 3. Phosphorus concentration at different soil depths in rice fields at the Sutiakhali cropland area

Depth (cm)	P concentration (mg kg^{-1})
10	7.70±1.98
20	5.53±1.3
30	4.99±1.28
40	3.36±1.66
50	3.25±0.56
60	3.69±1.31
70	2.93±0.86
80	3.47±1.31
90	3.14±1.84
100	2.49±1.63

The concentration decreased from 5.53 to 3.36 mg kg^{-1} between the 10-cm and 40-cm soil layers, but it did not vary significantly between 40 and 100 cm (Fig. 3 and Table 3). The plow pan was found in the 30-cm soil layer possibly retarded the downward movement of P. In addition, P did not move readily through the soil pore spaces because phosphate is highly reactive (Amin et al., 2021). Peng et al. (2011) stated that P is present in the soil as a negatively charged phosphate ion, which can readily bind with existing calcium, aluminum, iron, and other ions in the soil. This helps the P create new chemical compounds that are adsorbed tightly by the clay particle. Wortmann and Shapiro (2008) also found that a higher amount of P accumulated in the topsoil.

3.3. Pedotransfer function performance

The soil hydraulic properties estimated by the pedotransfer function matched well with the values optimized using the inverse modeling technique by the HYDRUS-1D model (Table 4). The hydraulic properties obtained through manual calibration against a set of observed soil water content data also agreed with the estimation of the pedotransfer function. The results suggest that the pedotransfer function can be confidently used to estimate the soil hydraulic properties in the location.

3.4. HYDRUS-1D model performance

A well-matched relationship was found between the observed and predicted soil water contents during the calibration and validation periods of the HYDRUS-1D modeling (Fig. 4). The performance indicators NSE and R^2 had values close to unity, and RMSE had lower values, which proved that the HYDRUS-1D model adequately predicted the field-scale hydrology of the study sites (Table 5). Thus, the validated HYDRUS-1D model was further used in this study to predict the effects of the altered soil hydraulic properties on the field-scale hydrology.

3.5. Soil hydraulic properties

3.5.1. Residual water content

Residual water content (θ_r) can be defined as the water content beyond which a further increase in the soil's suction results in only marginal changes in the water content (Šimůnek et al., 2009). It was maximum for the rice–rice rotation in the 10-cm soil layer for both sites (Fig. 5). In loam soil, the rice–rice rotation had the minimum θ_r in the plow pan (0.040 cm^3 cm^{-3}), followed by a gradual increase up to 0.047 cm^3 cm^{-3} in the 100-cm layer (Table 6). The plow pan layer had the minimum pore space, so it had a lower θ_r. In silt loam soil, the minimum θ_r was 0.037 cm^3 cm^{-3} in the 20-cm soil layer. In addition, the rice–rice and mixed crop rotations contained a similar θ_r along with the soil depth (Fig. 5b). The θ_r under the field ridge showed only a slight variation along the layers because the bulk densities also varied slightly from the top to the bottom layer (Fig. 5b and Table 7).

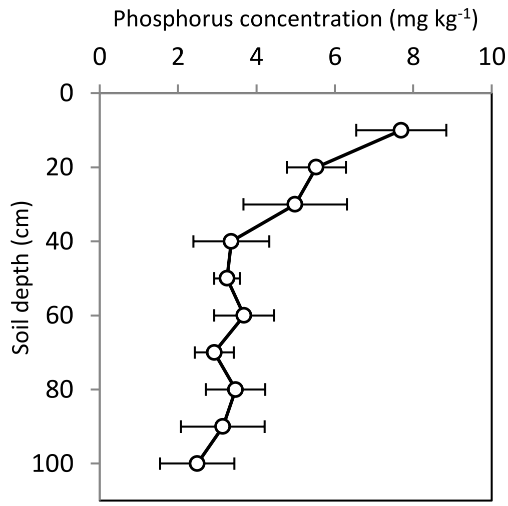

Figure 3. Phosphorus concentration at different depths in silt loam soil for rice–rice rotation

Table 4. Soil hydraulic properties predicted by different techniques

Process adapted	θ_r^* (cm^3 cm^{-3})	θ_s (cm^3 cm^{-3})	α (cm^{-1})	n	K_s (cm hr^{-1})	l
Pedotransfer function	0.049	0.42	0.006	1.64	3.6	0.5
Manual calibration	0.048	0.42	0.006	1.62	2.5	0.5
Inverse calibration	0.045	0.40	0.008	1.59	2.5	0.5

Note : *θ_r and θ_s are the residual and saturated water contents, respectively. α and n are empirical parameters determining the shape of the hydraulic functions. K_s is the saturated hydraulic conductivity, and l is the pore connectivity parameter.

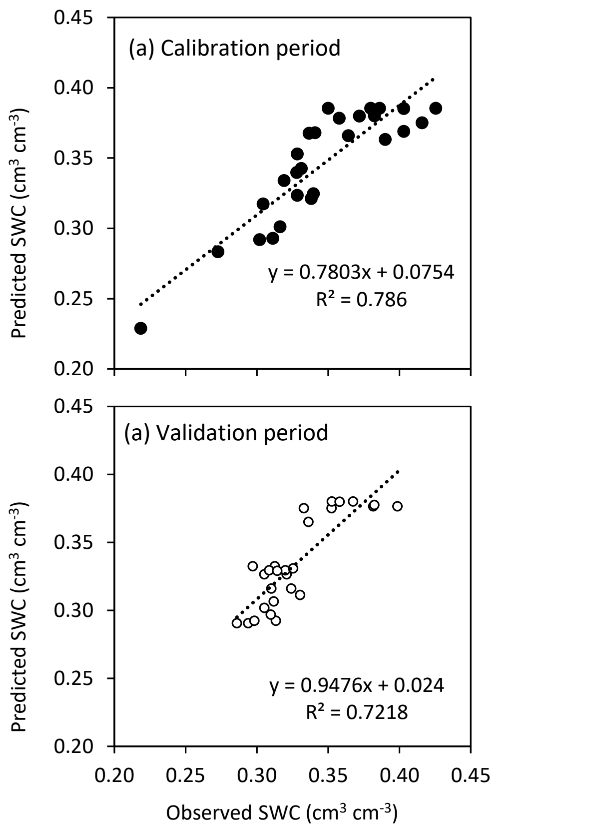

Figure 4. Agreement between the observed and predicted soil water contents (SWC) during the calibration and validation periods

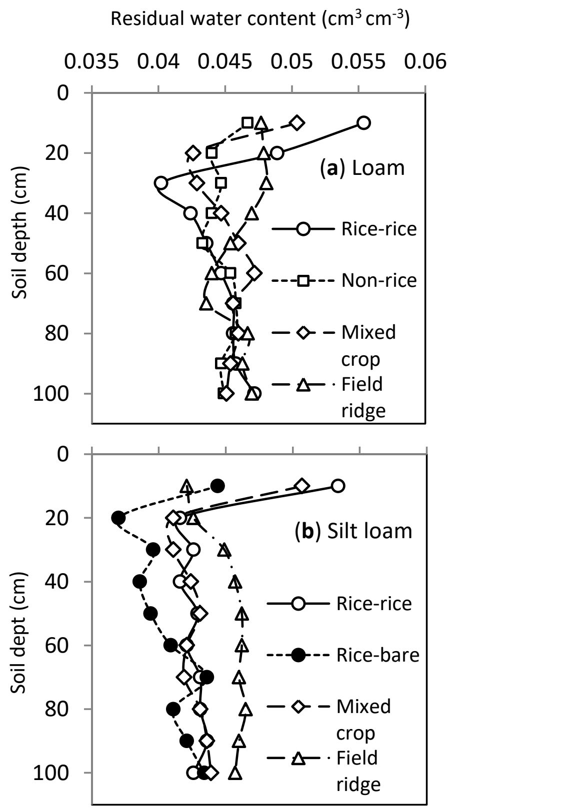

Figure 5. Residual soil water content at different soil depths for different crop rotations in (a) loam and (b) silt loam soil

3.5.2. Saturated water content

The saturated water content (θ_s) was higher in the 10 cm soil layer for both soils, and the rice–rice rotation had the highest value (Fig. 6). Higher saturated water content reduces the runoff loss but increases the percolation loss potential. In loam soil, the plow pan of the rice–rice rotation showed the lowest θ_s (0.344 cm^3 cm^{-3}) (Table 6). In silt loam soil, the plow pan layer of the rice-bare rotation had the minimum θ_s (0.339 cm^3 cm^{-3}), and the θ_s in the field ridge increased from 0.37 cm^3 cm^{-3} to 0.40 cm^3 cm^{-3} between the 10-cm and 30-cm soil layers (Table 7). Beyond the 30-cm soil layer, θ_s remained unchanged with depth (Fig. 6b).

Decayed rice roots and long-term puddling may be the reasons for the lower bulk density and higher θ_s in the topsoil of the rice–rice rotation. In addition, the relationship between bulk density and porosity probably affects the variation in θ_s among the soil layers. Leung et al. (2015) and Rajamanthri et al. (2021) stated that θ_s was higher in rooted soil than in unrooted soil. Kakaire et al. (2015) conducted a study in south central Uganda and revealed that soil porosity and bulk density are inversely related, with a decrease in one resulting in increasing the other.

Table 5. Performance indicators of the HYDRUS-1D model in predicting soil water contents during calibration and validation

Performance indicators	Calibration period	Validation period
NSE	0.786	0.596
RMSE (cm^3 cm^{-3})	0.021	0.018
CD	1.291	0.804
R^2	0.786	0.722

Note : NSE stands for Nash-Sutcliffe modeling efficiencies, RMSE root mean square error, CD coefficient of model determination, and R^2 coefficient of determination values (Moriasi et al., 2007).

3.5.3. Saturated hydraulic conductivity

The K_s in the topsoil layer for the rice–rice rotation was remarkably higher for both soil types. The values were 225.3 and 250.7 cm day^{-1} for loam and silt loam soil, respectively. In the loam soil, the plow pan of the rice–rice rotation had the lowest K_s (17.6 cm day^{-1}) (Fig. 7a and Table 6).

In silt loam soil, the minimum K_s was 26.9 cm day^{-1} in the 20-cm soil layer for the rice-bare rotation (Fig. 7b). The field ridge had the minimum K_s (58.3 cm day^{-1}) in the topsoil. Beyond the 30-cm soil layer, the K_s value remained unchanged (Fig. 7b). The K_s values for the rice–rice and mixed crop rotations were the same (Fig. 7b). The K_s under the field ridge was higher even in the 100 cm soil layer than other crop rotations (Table 7).

Bulk density influences the K_s. The K_s values can be related either directly (Yang et al., 2016a; Yang et al., 2016b) or inversely (Fu et al., 2015a; Fu et al., 2015b) to the bulk density. According to Fu et al. (2021), if the amount of macropores increases in proportion to the bulk density, K_s will also increase with the bulk density and vice versa. In addition, residual rice roots could be the reason behind the higher K_s in the topsoil. Marcacci et al. (2022) conducted a study and found that root age affects the relationship between K_s and roots in the soil. Shao et al. (2017), Bacq-Labreuil et al. (2019), and Lu et al. (2020) reported that K_s and macroporosity increased due to the presence of decayed roots in the soil.

3.6. Model predicted hydrology

3.6.1. Runoff

In both soil types, the runoff rate was found to be the lowest in the field ridge among the crop rotations. For a 3.33 cm hr^{-1} rainfall event in silt loam soil, the field ridge produced no runoff (Fig. 8d).

However, for 5 cm hr^{-1} and 6.66 cm hr^{-1} rainfall events, the runoff was generated over the field ridge with maximum rates of 1.69 cm hr^{-1} and 3.36 cm hr^{-1}, respectively, during the first hour of rainfall (Fig. 8e, f). In addition, the runoff rates were higher in loam soil than in silt loam because the bulk density of the loam soil was higher (Fig. 8).

The maximum runoff rates in loam and silt loam soil were for the mixed crop and rice-bare rotation, respectively (Fig. 8). For the 6.66 cm hr^{-1} rainfall event, the runoff rate at the first hour for the mixed-crop rotation in loam soil was 5.55 cm hr^{-1} (Fig. 8c), whereas it was 5.45 cm hr^{-1} for the rice-bare rotation in silt loam soil (Fig. 8f). In addition, the rice–rice and non-rice rotations had an approximately similar runoff rate for the rainfall events.

3.6.2. Infiltration

The field ridge in both soil types had the highest infiltration rate because it had the maximum average hydraulic conductivity throughout the soil layers among all crop rotations (Fig. 9). The lowest infiltration was observed under the mixed crop rotation in the loam soil and under the rice-bare rotation in silt loam soil. This may be due to the overall lower hydraulic conductivity in the upper soil layers of these two crop rotations. The rice–rice rotation had the second highest infiltration rate for both soil types (Fig. 9). The higher K_s in the topsoil of the rice–rice rotation facilitated the infiltration rate.

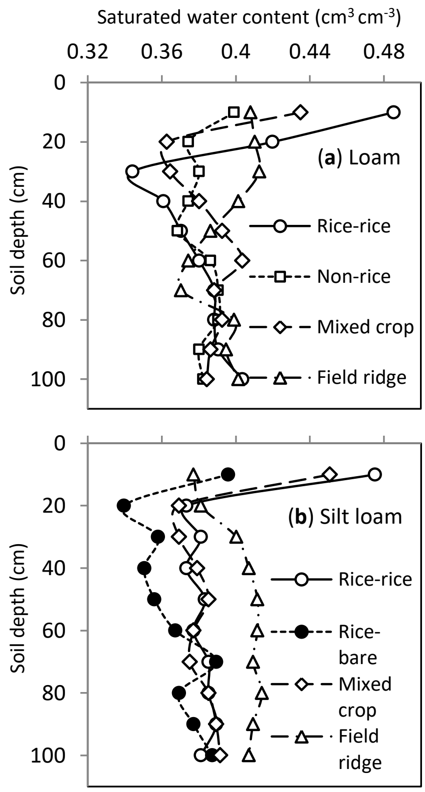

Figure 6. Saturated water content at different soil depths for different crop rotations in (a) loam and (b) silt loam soil

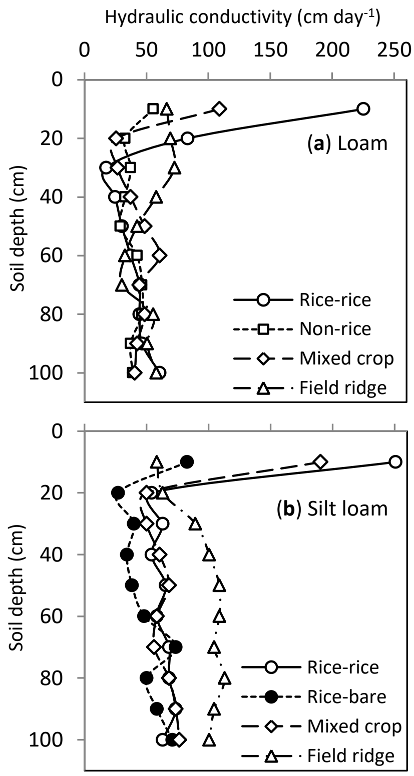

Figure 7. Saturated hydraulic conductivity (K_s) at different soil depths for different crop rotations in (a) loam and (b) silt loam soil

Table 6. Hydraulic properties of loam soil at the Bangladesh Agricultural University farm area

Saturated hydraulic conductivity (cm day^{-1})				Saturated water content (cm^3 cm^{-3})				Residual water content (cm^3 cm^{-3})				Depth from soil surface
Field ridge	Mixed crop	Non-rice	Rice-rice	Field ridge	Mixed crop	Non-rice	Rice-rice	Field ridge	Mixed crop	Non-rice	Rice-rice	cm
66.440	108.930	55.480	225.350	0.408	0.435	0.399	0.485	0.048	0.050	0.047	0.055	10
69.510	25.670	32.800	83.250	0.410	0.363	0.374	0.420	0.048	0.043	0.044	0.049	20
72.720	26.720	37.270	17.560	0.413	0.365	0.380	0.344	0.048	0.043	0.045	0.040	30
58.040	37.270	32.800	24.680	0.401	0.380	0.374	0.361	0.047	0.045	0.044	0.042	40
42.470	48.500	28.970	30.180	0.386	0.393	0.369	0.370	0.045	0.046	0.043	0.044	50
32.800	60.710	42.470	37.270	0.374	0.404	0.386	0.380	0.044	0.047	0.045	0.045	60
30.180	44.380	46.390	44.380	0.370	0.388	0.391	0.388	0.044	0.046	0.046	0.046	70
55.480	48.500	46.390	44.380	0.399	0.393	0.391	0.388	0.047	0.046	0.046	0.046	80
50.720	42.470	37.270	46.390	0.395	0.386	0.380	0.391	0.046	0.045	0.045	0.046	90
58.040	40.650	38.910	60.710	0.401	0.384	0.382	0.404	0.047	0.045	0.045	0.047	100

Table 7. Hydraulic properties of silt loam soil at the Sutiakhali cropland area

Saturated hydraulic conductivity (cm day^{-1})				Saturated water content (cm^3 cm^{-3})				Residual water content (cm^3 cm^{-3})				Depth from soil surface
Field ridge	Mixed crop	Non-rice	Rice-rice	Field ridge	Mixed crop	Non-rice	Rice-rice	Field ridge	Mixed crop	Non-rice	Rice-rice	cm
58.320	190.340	82.740	250.700	0.377	0.451	0.396	0.475	0.042	0.051	0.044	0.053	10
63.000	50.030	26.970	54.000	0.381	0.369	0.340	0.373	0.043	0.041	0.037	0.042	20
89.460	50.030	39.790	63.000	0.400	0.369	0.358	0.381	0.045	0.041	0.040	0.043	30
100.560	60.610	34.120	54.000	0.407	0.379	0.351	0.373	0.046	0.042	0.039	0.042	40
108.680	68.080	38.290	65.490	0.412	0.385	0.356	0.383	0.046	0.043	0.039	0.043	50
108.680	58.320	48.150	58.320	0.412	0.377	0.367	0.377	0.046	0.042	0.041	0.042	60
104.550	56.120	73.590	68.080	0.409	0.375	0.389	0.385	0.046	0.042	0.044	0.043	70
112.960	68.080	50.030	68.080	0.414	0.385	0.369	0.385	0.047	0.043	0.041	0.043	80
104.550	73.590	58.320	73.590	0.409	0.389	0.377	0.389	0.046	0.044	0.042	0.044	90
100.560	76.520	70.780	63.000	0.407	0.392	0.387	0.381	0.046	0.044	0.043	0.043	100

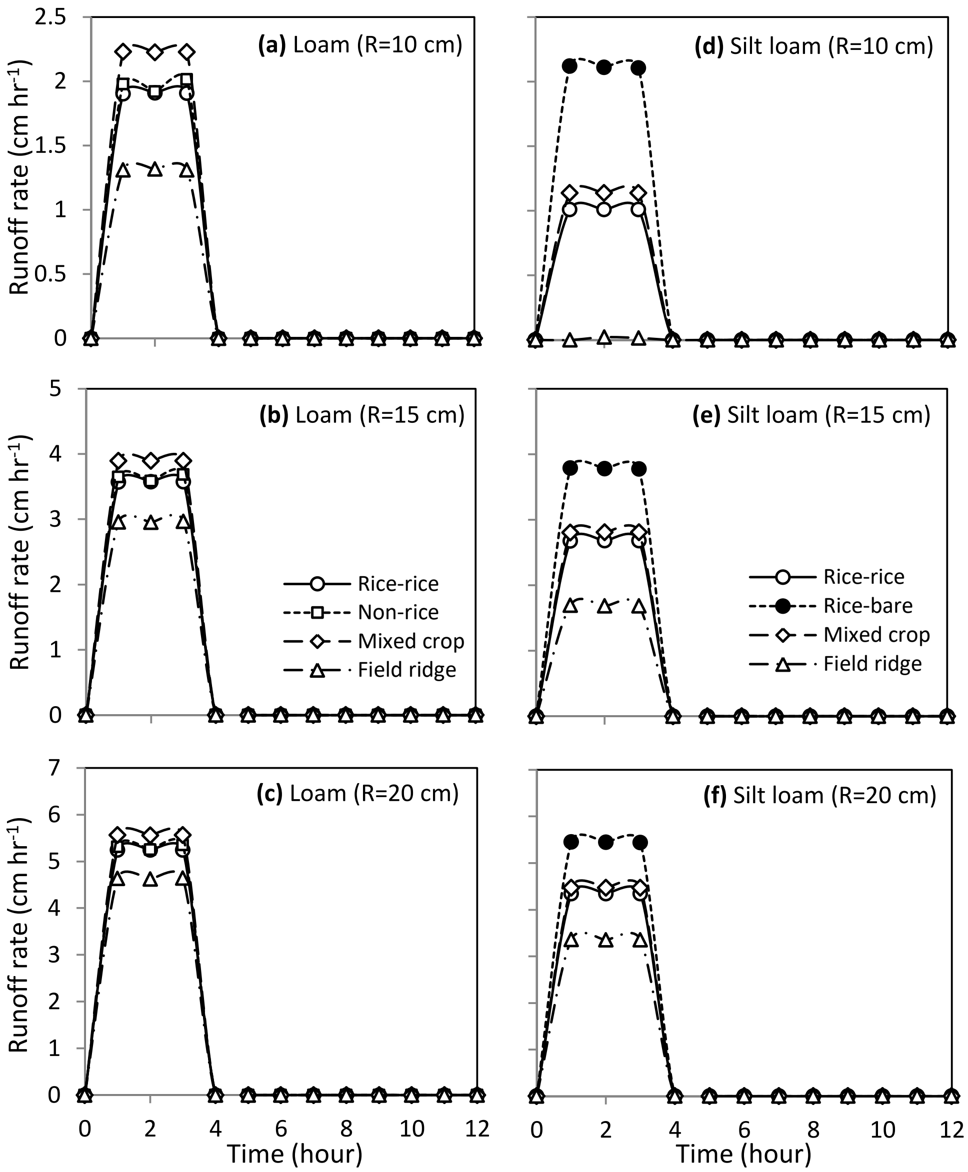

Figure 8. Runoff rate for different crop rotations in (a) loam and (b) silt loam soil (R stands for rainfall)

The silt loam soil had a higher infiltration rate than the loam soil for all the crop rotations except for the rice-bare field. The cumulative infiltration in the silt loam soil was 2.27 cm, 3.26 cm, and 3.7 cm higher than that in the loam soil for the rice–rice, mixed crop, and field ridge rotations, respectively (Fig. 9). The loam soil should have a higher infiltration rate than the silt loam soil, but the higher bulk density of the loam soil reduced its infiltration capacity. Wang et al. (2015) conducted a rainfall-infiltration simulation study with 9 and 12 cm hr^{-1} rainfall events in fluvo-aquic soil and found infiltration rates of 6.45 and 8.47 cm hr^{-1}, respectively, in bare soil and 6.95 and 9.43 cm hr^{-1} in cultivated soil.

3.6.3. Percolation

The field ridge showed a higher percolation rate than the other crop rotations for both soil types because the maximum infiltration occurred through the field ridge. Moreover, the field ridge had higher percolation in the silt loam soil than that in the loam soil during the simulation period (Fig. 10).

The rice–rice rotation in the loam soil showed the second highest percolation, although it had a well-developed plow pan (Fig. 10). The higher hydraulic conductivity in the top 10-cm soil layer of the rice–rice rotation facilitated infiltration and retarded runoff generation, thereby increasing water storage and percolation. In loam soil, the minimum percolation occurred through the mixed crop field, while the minimum percolation for the silt loam soil occurred in the rice-bare field. The silt loam soil had a higher cumulative percolation than the loam soil (Fig. 10).

Soil physical properties and rainfall intensity affect the percolation rate. Xu et al. (2019) stated that percolation is directly related to the K_s of the soil. Xu et al. (2019) experimented with a terrace field in Zhanghe Irrigation District, China, where field ridge soil properties were made identical to the paddy field and found that percolation occurred in the paddy field with values between 23.2 and 31.3% water application. In addition, 10.5–14.8% of applied water was lost through the field ridge by percolation and lateral seepage. Amin et al. (2021) conducted a study in lysimeters containing silt loam soil and reported that 38–44% of the total water input was lost by percolation from rain-fed Aman fields.

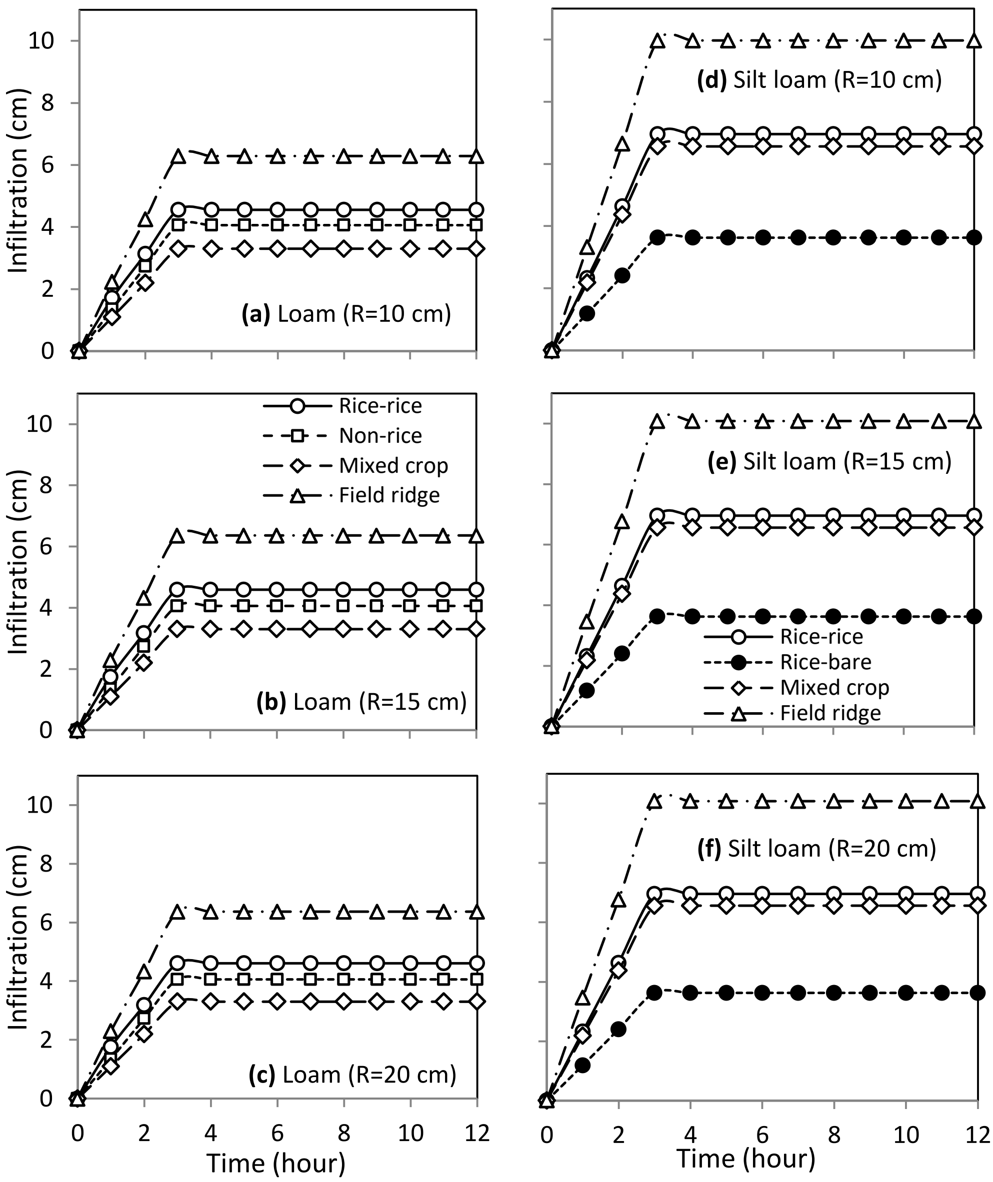

Figure 9. Infiltration for different crop rotations in (a) loam and (b) silt loam soil

4. DISCUSSION

The soil bulk density gradually increased from the soil surface to the plow pan layer at 20–30 cm depth for most of the land management options but did not vary significantly below the plow pan layer. Kar et al. (2023b) conducted a study in India's North-West Himalayan region to investigate sustainable tillage techniques and found that soil bulk density increased along with the depth. Mehler et al. (2014) and Liu et al. (2020) also stated a similar trend of soil bulk density along with depth. This can be explained by the fact that the frequent tillage operation by heavy farming equipment (Patra et al., 2019) at the same depth for a long time resulted in the subsurface (20–30 cm depth) soil compaction and increased soil bulk density (Havaee et al., 2014).

The rice–rice rotation formed a well-developed plow pan at 20–30 cm with the highest bulk density among the land-management options in loam soil. The mixed crop field also developed a moderate plow pan. Tillage operations in the rice fields crushed the topsoil formation and reduced the bulk density, but this altered the soil physical properties in the subsurface soil layer between 20 and 30 cm depth by compaction. As a result, a plow pan was formed in this subsurface layer. Shah et al. (2017) also stated that tillage operations result in sub-soil (20–30 cm) compaction that reduces the soil porosity and increases soil bulk density which helps develop a crust below the tilled layer, a plow pan. However, no plow pan was formed under the field ridge because this part of the land did not receive puddling or tillage.

The top 10 cm soil layer in the rice–rice rotation had remarkably lower bulk density with maximum effective porosity and higher K_s, which helped store more water above the plow pan layer. Mairghany et al. (2019) reported that repeated tillage operation decreased the soil bulk density and increased the porosity and particle density at the 0-20 cm soil layer. Lower bulk density can improve water storage capacity in the tilled layer (Amin et al., 2014). As a result, the stored water in this layer subsequently percolated through the plow pan layer. This was the reason for the higher percolation in the rice–rice rotation than in the mixed crop rotation.

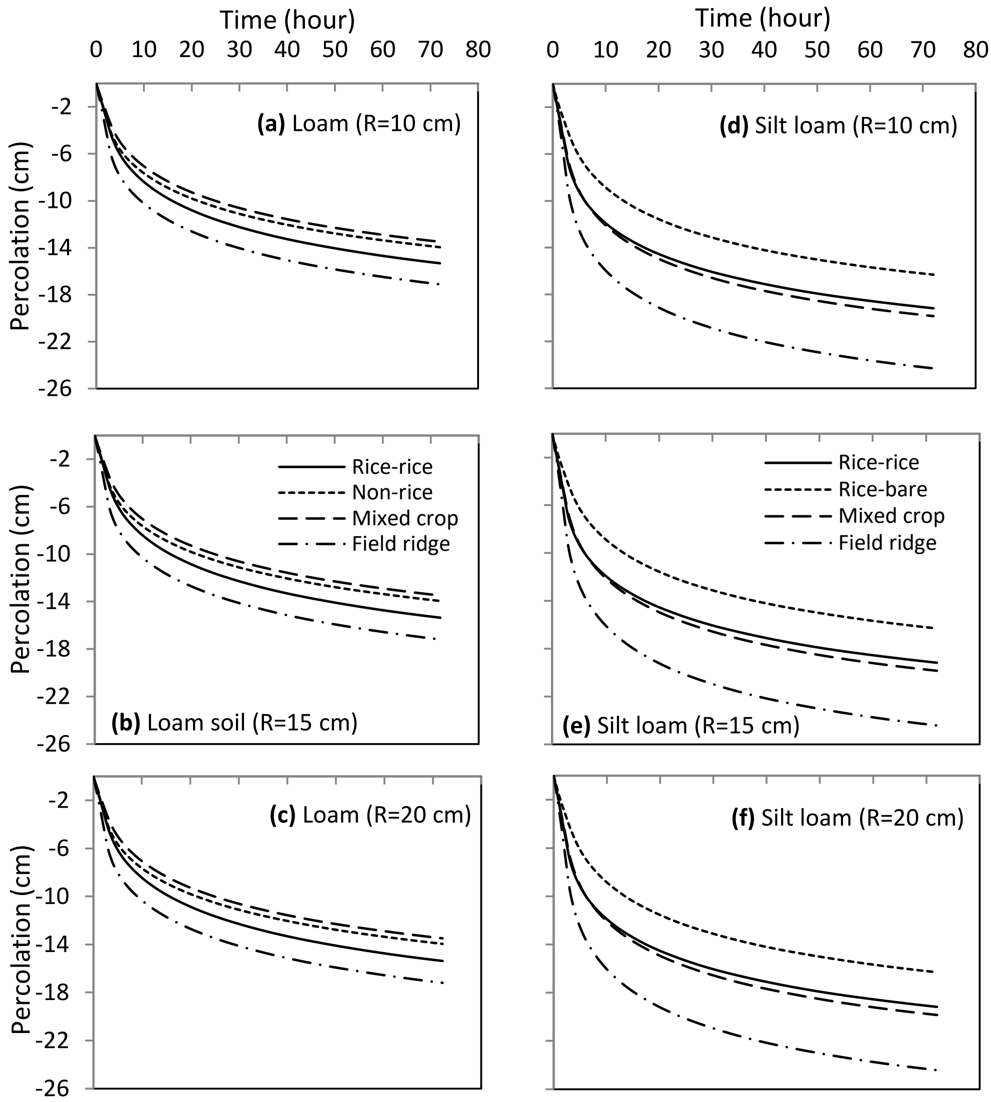

Figure 10. Percolation for different crop rotations in (a) loam and (b) silt loam soil

The rice-bare rotation also had a plow pan layer because the field was previously used to cultivate rice crops. The field was kept fallow for the last four years, which caused the relatively higher bulk density in the topsoil also. Consequently, the rice-bare rotation had lower infiltration and percolation in the topsoil than the ongoing rice–rice rotation. As tillage operation was absent in recent years, the topsoil got time to get settled with increased bulk density (Nawaz et al., 2013; de Moraes et al., 2016). Tillage operations loosen topsoil, but the loose soil starts to collapse gradually due to gravity, rainfall, and water infiltration through the soil profile (Bogunovic et al., 2018). Moreover, the soil settlement in the top layer can be expedited by the kinetic energy of rainfall (Nanko et al., 2015). The topsoil aggregates can be broken by raindrop impact, and the continuous breakdown and dispersion of soil aggregates can release minute soil particles, which can reduce the number of macro pores and lower saturated hydraulic conductivity (Wang et al., 2015). Osunbitan et al. (2005) stated that the bulk density was increased by 55–61% in surface soil (0–15 cm) 8 weeks after tillage operation. Bogunovic et al. (2018) conducted a study in Croatia at 45° 56′ N, 17° 02′ E at 129 m above sea level to investigate the impacts of different tillage operations on soil compaction and found that no-tillage increased the soil bulk density in the 0-10 cm soil depth by approximately 8% compared to conventional tillage. Gao et al. (2016) conducted a study in clay loam soil and found that the soil bulk density was higher after 3 years of no-tillage compared to tilled soil. Singh et al. (2016) also found similar results on clay loam soils in India.

The P concentration decreased rapidly between the 10 cm and 40 cm soil layers but did not vary significantly below the 40 cm soil layer. This may be caused due to the presence of a plow pan which may impede the downward movement of P. However, P transportation can also be affected by the impact of colloid particles present in the subsoil (Pang et al., 2016), namely, clay minerals, metal oxides, and bio-colloids (protozoa, viruses, and bacteria) (Jiang et al., 2021). Moreover, phosphorus accumulation in soils has a direct relationship with the amount of existing iron oxides, aluminum oxides, and aluminosilicate minerals (Jiang et al., 2021; Scalenghe et al., 2014). In addition, preferential flow channels can also act as pathways for phosphorus movement (Chen & Arai, 2020; Toor & Sims, 2015). However, all of that can be affected by the plow pan in the rice fields.

The HYDRUS-1D simulation results show that the soil hydraulic properties and rainfall intensities affect the runoff rate. Wang et al. (2015) simulated three rainfall events (6 cm hr^{-1}, 9 cm hr^{-1}, and 12 cm hr^{-1}) for bare and cultivated soils and stated that no runoff was generated during the 6 cm rainfall event, but less than 3.6 cm hr^{-1} runoff was generated during the 9 cm and 12 cm rainfall events in both soils.

The loam soil was supposed to have a higher infiltration and percolation rate than the silt loam soil, but in our experiment, the result was the opposite. The silt loam soil had a lower bulk density and thereby higher hydraulic conductivity than the loam soil, which facilitated infiltration and percolation through the silt loam soil. The minimum runoff and maximum amount of percolation through the field ridge were predicted by the HYDRUS-1D, which indicates that the field ridge was the main pathway of water loss in rice fields. The average hydraulic conductivity in the field ridges was higher, which caused higher percolation. This can be explained by the fact that the field ridge area had higher and uniform hydraulic conductivity due to the absence of a plow pan. Janssen and Lennartz (2009) conducted a study in southeastern China and reported that the hydraulic conductivity below the field ridge was remarkably greater than that in the main rice field because the field ridge is not puddled during the tillage operation. In such a situation, water can move horizontally over the plow pan and route to the field ridge before moving downward, which may go unnoticed. Huang et al. (2003) also agreed with these findings. This result suggests that interventions are needed to retard this water loss pathway in rice fields. The findings of this experiment will help assess the potential pathway of water loss and understand the field-scale hydrology of the crop rotations. Further study is needed to validate the findings for more soil types. A larger volume of soil core sampling would help understand the effects of cracks and fissures usually developed in rice fields on the soil hydraulic properties and hydrology. In situ measurements of some soil hydraulic properties can be performed in further studies.

5. CONCLUSION

The rice–rice rotation had a well-developed plow pan in the 30 cm soil layer, but the topsoil had lower bulk density and higher infiltration capacity. Therefore, this rotation had higher soil water storage in the topsoil (0-20 cm) and thus higher subsequent percolation than the mixed crop rotation. Such a plow pan was not developed under the field ridge, so it had a higher percolation rate. As a result, the field ridge of a rice field can be the main water loss pathway. The findings of this study will help assess the potential water loss pathways and manage both soil and water more efficiently to reduce the yield gaps of different crops.

Acknowledgments

The Bangladesh Agricultural University, Mymensingh, Bangladesh (Project No.: 2021/80/BAU; Title: Water security, soil hydraulic properties and yield response to maize crop introduction into a rice–rice rotation) supported this research work.

Declaration of Competing Interest

The authors declare that no competing financial or personal interests that may appear and influence the work reported in this paper.

References

Ali, M., Amin, M. G. M., & Islam, A. (2005). Reference crop evapo-transpiration (ET0) over Bangladesh and its implication in crop planning. *Journal of the Bangladesh Agricultural University*, *3*(452-2018-3816), 139-147. https://doi.org/10.22004/ag.econ.276419.

Amin, M., Khan, M. J., Jan, M. T., Rehman, M. U., Tariq, J. A., Hanif, M., & Shah, Z. (2014). Effect of different tillage practices on soil physical properties under wheat in semi-arid environment. *Soil and Environment*, *33*(1), 33-37. http://www.se.org.pk/File-Download.aspx?archivedpaperid=712.

Amin, M. G. M., Akter, A., Jahangir, M. M. R., & Ahmed, T. (2021). Leaching and runoff potential of nutrient and water losses in rice field as affected by alternate wetting and drying irrigation. *Journal of Environmental Management*, *297*, 113402. https://doi.org/10.1016/j.jenvman.2021.113402.

Amin, M. G. M., Pedersen, C. Ø., Forslund, A., Veith, T. L., & Laegdsmand, M. (2016). Influence of soil structure on contaminant leaching from injected slurry. *Journal of Environmental Management*, *184*, 289-296. https://doi.org/10.1016/j.jenvman.2016.10.002.

Amin, M. G. M., Šimůnek, J., & Lægdsmand, M. (2014). Simulation of the redistribution and fate of contaminants from soil-injected animal slurry. *Agricultural Water Management*, *131*, 17-29. https://doi.org/10.1016/j.agwat.2013.09.002.

Bacq-Labreuil, A., Crawford, J., Mooney, S. J., Neal, A. L., & Ritz, K. (2019). Cover crop species have contrasting influence upon soil structural genesis and microbial community phenotype. *Scientific Reports*, *9*(1), 7473. https://doi.org/10.1038/s41598-019-43937-6.

Bogunovic, I., Pereira, P., Kisic, I., Sajko, K., & Sraka, M. (2018). Tillage management impacts on soil compaction, erosion and crop yield in Stagnosols (Croatia). *CATENA*, *160*, 376-384. https://doi.org/10.1016/j.catena.2017.10.009.

Cabangon, R. J., Tuong, T. P., Castillo, E. G., Bao, L. X., Lu, G., Wang, G., Cui, Y., Bouman, B. A. M., Li, Y., Chen, C., & Wang, J. (2004). Effect of irrigation method and N-fertilizer management on rice yield, water productivity and nutrient-use efficiencies in typical lowland rice conditions in China. *Paddy and Water Environment*, *2*(4), 195-206. https://doi.org/10.1007/s10333-004-0062-3.

Carrijo, D. R., Lundy, M. E., & Linquist, B. A. (2017). Rice yields and water use under alternate wetting and drying irrigation: A meta-analysis. *Field Crops Research*, *203*, 173-180. https://doi.org/10.1016/j.fcr.2016.12.002.

Chauhan, B. S., Jabran, K., & Mahajan, G. (Eds.). (2017). *Rice Production Worldwide*. Springer International Publishing. https://doi.org/10.1007/978-3-319-47516-5.

Chen, A., & Arai, Y. (2020). Chapter Three - Current uncertainties in assessing the colloidal phosphorus loss from soil. In D. L. Sparks (Ed.), *Advances in Agronomy* (Vol. 163, pp. 117-151). Academic Press. https://doi.org/10.1016/bs.agron.2020.05.002

Chen, G., Weil, R. R., & Hill, R. L. (2014). Effects of compaction and cover crops on soil least limiting water range and air permeability. *Soil and Tillage Research*, *136*, 61-69. https://doi.org/10.1016/j.still.2013.09.004.

Chen, S. K., & Liu, C. W. (2002). Analysis of water movement in paddy rice fields (I) experimental studies. *Journal of Hydrology*, *260*(1), 206-215. https://doi.org/10.1016/S0022-1694(01)00615-1.

Datta, A., Ullah, H., & Ferdous, Z. (2017). Water Management in Rice. In B. S. Chauhan, K. Jabran, & G. Mahajan (Eds.), *Rice Production Worldwide* (pp. 255-277). Springer International Publishing. https://doi.org/10.1007/978-3-319-47516-5_11

Fang, J., Zhang, K., Sun, P., Lin, D., Shen, B., & Luo, Y. (2016). Co-transport of Pb2+ and TiO2 nanoparticles in repacked homogeneous soil columns under saturation condition: Effect of ionic strength and fulvic acid. *Science of The Total Environment*, *571*, 471-478. https://doi.org/10.1016/j.scitotenv.2016.07.013.

FAO. (2020). World food and agriculture - statistical yearbook 2020. *World Food and Agriculture-Statistical Yearbook*. https://doi.org/10.4060/cb1329en.

Fu, T., Chen, H., Zhang, W., Nie, Y., Gao, P., & Wang, K. (2015a). Spatial variability of surface soil saturated hydraulic conductivity in a small karst catchment of southwest China. *Environmental Earth Sciences*, *74*(3), 2381-2391. https://doi.org/10.1007/s12665-015-4238-5.

Fu, T., Chen, H., Zhang, W., Nie, Y., & Wang, K. (2015b). Vertical distribution of soil saturated hydraulic conductivity and its influencing factors in a small karst catchment in Southwest China. *Environmental Monitoring and Assessment*, *187*(3), 92. https://doi.org/10.1007/s10661-015-4320-1.

Fu, T., Gao, H., Liang, H., & Liu, J. (2021). Controlling factors of soil saturated hydraulic conductivity in Taihang Mountain Region, northern China. *Geoderma Regional*, *26*, e00417. https://doi.org/10.1016/j.geodrs.2021.e00417.

Gao, W., Whalley, W. R., Tian, Z., Liu, J., & Ren, T. (2016). A simple model to predict soil penetrometer resistance as a function of density, drying and depth in the field. *Soil and Tillage Research*, *155*, 190-198. https://doi.org/10.1016/j.still.2015.08.004.

Havaee, S., Ayoubi, S., Mosaddeghi, M. R., & Keller, T. (2014). Impacts of land use on soil organic matter and degree of compactness in calcareous soils of central Iran. *Soil Use and Management*, *30*(1), 2-9. https://doi.org/10.1111/sum.12092.

He, Y., Lehndorff, E., Amelung, W., Wassmann, R., Alberto, M. C., von Unold, G., & Siemens, J. (2017). Drainage and leaching losses of nitrogen and dissolved organic carbon after introducing maize into a continuous paddy-rice crop rotation. *Agriculture, Ecosystems & Environment*, *249*, 91-100. https://doi.org/10.1016/j.agee.2017.08.021.

Huang, H. C., Liu, C. W., Chen, S. K., & Chen, J. S. (2003). Analysis of percolation and seepage through paddy bunds. *Journal of Hydrology*, *284*(1), 13-25. https://doi.org/10.1016/S0022-1694(03)00228-2.

Islam, M. D. D., Price, A. H., & Hallett, P. D. (2021). Contrasting ability of deep and shallow rooting rice genotypes to grow through plough pans containing simulated biopores and cracks. *Plant and Soil*, *467*(1), 515-530. https://doi.org/10.1007/s11104-021-05131-4.

Islam, M. M., Meerschman, E., Saey, T., De Smedt, P., Van De Vijver, E., Delefortrie, S., & Van Meirvenne, M. (2014). Characterizing Compaction Variability with an Electromagnetic Induction Sensor in a Puddled Paddy Rice Field. *Soil Science Society of America Journal*, *78*(2), 579-588. https://doi.org/10.2136/sssaj2013.07.0289.

Talukolaee, M. J., Darzi Naftchali, A., Parvariji, L. Z., & Ahmadi, M. Z. (2018). Investigating long-term effects of subsurface drainage on soil structure in paddy fields. *Soil and Tillage Research*, *177*, 155-160. https://doi.org/10.1016/j.still.2017.12.012.

Janssen, M., & Lennartz, B. (2009). Water losses through paddy bunds: Methods, experimental data, and simulation studies. *Journal of Hydrology*, *369*(1), 142-153. https://doi.org/10.1016/j.jhydrol.2009.02.038.

Jiang, B., Shen, J., Sun, M., Hu, Y., Jiang, W., Wang, J., Li, Y., & Wu, J. (2021). Soil phosphorus availability and rice phosphorus uptake in paddy fields under various agronomic practices. *Pedosphere*, *31*(1), 103-115. https://doi.org/10.1016/S1002-0160(20)60053-4.

Kakaire, J., Makokha, G. L., Mwanjalolo, M., Mensah, A. K., & Menya, E. (2015). Effects of Mulching on Soil Hydro-Physical Properties in Kibaale Sub-catchment, South Central Uganda. *Applied Ecology and Environmental Sciences*, *3*(5), 127-135. https://doi.org/10.12691/aees-3-5-1.

Kar, S. K., Patra, S., Singh, R. M., Sankar, M., Kumar, S., Singh, D., Madhu, M.,& Singla, S. (2023a). Impact of land use reformation on soil hydraulic properties and recovery potential of conservation tillage in India's North-West Himalayan region. *Ecohydrology & Hydrobiology*, *23*(2), 290-303. https://doi.org/10.1016/j.ecohyd.2022.12.008.

Kar, S. K., Singh, R. M., Patra, S., Sankar, M., Kumar, S., & Singh, A. (2023b). Implication of land use shifting on land degradation and restoration potential of conservation agriculture in India's North-West Himalayan region. *Geoderma Regional*, *32*, e00616. https://doi.org/10.1016/j.geodrs.2023.e00616.

Kirkham, J. M., Smith, C. J., Doyle, R. B., & Brown, P. H. (2019). Inverse modelling for predicting both water and nitrate movement in a structured-clay soil (Red Ferrosol). *PeerJ*, *6*, e6002. https://doi.org/10.7717/peerj.6002.

Leung, A. K., Garg, A., & Ng, C. W. W. (2015). Effects of plant roots on soil-water retention and induced suction in vegetated soil. *Engineering Geology*, *193*, 183-197. https://doi.org/10.1016/j.enggeo.2015.04.017.

Li, Y., Šimůnek, J., Jing, L., Zhang, Z., & Ni, L. (2014). Evaluation of water movement and water losses in a direct-seeded-rice field experiment using Hydrus-1D. *Agricultural Water Management*, *142*, 38-46. https://doi.org/10.1016/j.agwat.2014.04.021.

Liu, Q., Kan, Z., He, C., & Zhang, H. (2020). Effects of Strategic Tillage on Soil Physicochemical Properties and Grain Yield in the North China Plain. *Agronomy*, *10*(8), 1167. https://doi.org/10.3390/agronomy10081167.

Lu, J., Zhang, Q., Werner, A. D., Li, Y., Jiang, S., & Tan, Z. (2020). Root-induced changes of soil hydraulic properties – A review. *Journal of Hydrology*, *589*, 125203. https://doi.org/10.1016/j.jhydrol.2020.125203.

Mairghany, M., Yahya, A., Adam, N. M., Su, A. S. M., Aimrun, W., & Elsoragaby, S. (2019). Rotary tillage effects on some selected physical properties of fine textured soil in wetland rice cultivation in Malaysia. *Soil and Tillage Research*, *194*, 104318. https://doi.org/10.1016/j.still.2019.104318.

Marcacci, K. M., Warren, J. M., Perfect, E., & Labbé, J. L. (2022). Influence of living grass Roots and endophytic fungal hyphae on soil hydraulic properties. *Rhizosphere*, *22*, 100510. https://doi.org/10.1016/j.rhisph.2022.100510.

McCarty, L. B., Hubbard, L. R., & Quisenberry, V. L. (2016). *Applied soil physical properties, drainage, and irrigation strategies*. Springer. https://doi.org/10.1007/978-3-319-24226-2

Mehler, K., Schöning, I., & Berli, M. (2014). The Importance of Rock Fragment Density for the Calculation of Soil Bulk Density and Soil Organic Carbon Stocks. *Soil Science Society of America Journal*, *78*(4), 1186-1191. https://doi.org/10.2136/sssaj2013.11.0480.

Mo'allim, A. A., Kamal, M. R., Muhammed, H. H., Yahaya, N. K. E. M., Zawawe, M. A. b. M., Man, H. B. C., & Wayayok, A. (2018). An Assessment of the Vertical Movement of Water in a Flooded Paddy Rice Field Experiment Using Hydrus-1D. *Water*, *10*(6), 783. https://doi.org/10.3390/w10060783.

Mondal, S., Kumar, S., Haris, A. A., Dwivedi, S. K., Bhatt, B. P., & Mishra, J. S. (2016). Effect of different rice establishment methods on soil physical properties in drought-prone, rainfed lowlands of Bihar, India. *Soil Research*, *54*(8), 997-1006. https://doi.org/10.1071/SR15346.

Moriasi, D. N., Arnold, J. G., Van Liew, M. W., Bingner, R. L., Harmel, R. D., & Veith, T. L. (2007). Model Evaluation Guidelines for Systematic Quantification of Accuracy in Watershed Simulations. *Transactions of the ASABE*, *50*(3), 885-900. https://doi.org/10.13031/2013.23153.

Nanko, K., Giambelluca, T. W., Sutherland, R. A., Mudd, R. G., Nullet, M. A., & Ziegler, A. D. (2015). Erosion Potential under Miconia calvescens Stands on the Island of Hawai'i. *Land Degradation & Development*, *26*(3), 218-226. https://doi.org/10.1002/ldr.2200.

Nawaz, M. F., Bourrié, G., & Trolard, F. (2013). Soil compaction impact and modelling. A review. *Agronomy for Sustainable Development*, *33*(2), 291-309. https://doi.org/10.1007/s13593-011-0071-8.

Neumann, R. B., Polizzotto, M. L., Badruzzaman, A. B. M., Ali, M. A., Zhang, Z., & Harvey, C. F. (2009). Hydrology of a groundwater-irrigated rice field in Bangladesh: Seasonal and daily mechanisms of infiltration. *Water Resources Research*, *45*(9). https://doi.org/10.1029/2008WR007542.

Osunbitan, J. A., Oyedele, D. J., & Adekalu, K. O. (2005). Tillage effects on bulk density, hydraulic conductivity and strength of a loamy sand soil in southwestern Nigeria. *Soil and Tillage Research*, *82*(1), 57-64. https://doi.org/10.1016/j.still.2004.05.007.

Pang, L., Lafogler, M., Knorr, B., McGill, E., Saunders, D., Baumann, T., Abraham, P., & Close, M. (2016). Influence of colloids on the attenuation and transport of phosphorus in alluvial gravel aquifer and vadose zone media. *Science of The Total Environment*, *550*, 60-68. https://doi.org/10.1016/j.scitotenv.2016.01.075.

Patil, M. D., & Das, B. S. (2013). Assessing the effect of puddling on preferential flow processes through under bund area of lowland rice field. *Soil and Tillage Research*, *134*, 61-71. https://doi.org/10.1016/j.still.2013.07.008.

Patra, S., Julich, S., Feger, K. H., Jat, M. L., Jat, H., Sharma, P. C., & Schwärzel, K. (2019). Soil hydraulic response to conservation agriculture under irrigated intensive cereal-based cropping systems in a semiarid climate. *Soil and Tillage Research*, *192*, 151-163. https://doi.org/10.1016/j.still.2019.05.003.

Peng, S. Z., Yang, S. H., Xu, J. Z., Luo, Y. F., & Hou, H. J. (2011). Nitrogen and phosphorus leaching losses from paddy fields with different water and nitrogen managements. *Paddy and Water Environment*, *9*(3), 333-342. https://doi.org/10.1007/s10333-010-0246-y.

Pereira, L. S., Cordery, I., & Iacovides, I. (2012). Improved indicators of water use performance and productivity for sustainable water conservation and saving. *Agricultural Water Management*, *108*, 39-51. https://doi.org/10.1016/j.agwat.2011.08.022.

Phogat, V., Skewes, M. A., McCarthy, M. G., Cox, J. W., Šimůnek, J., & Petrie, P. R. (2017). Evaluation of crop coefficients, water productivity, and water balance components for wine grapes irrigated at different deficit levels by a sub-surface drip. *Agricultural Water Management*, *180*, 22-34. https://doi.org/10.1016/j.agwat.2016.10.016.

Rajamanthri, K., Jotisankasa, A., & Aramrak, S. (2021). Effects of Chrysopogon zizanioides root biomass and plant age on hydro-mechanical behavior of root-permeated soils. *International Journal of Geosynthetics and Ground Engineering*, *7*(2), 36. https://doi.org/10.1007/s40891-021-00271-0.

Scalenghe, R., Edwards, A. C., Barberis, E., & Ajmone-Marsan, F. (2014). Release of phosphorus under reducing and simulated open drainage conditions from overfertilised soils. *Chemosphere*, *95*, 289-294. https://doi.org/10.1016/j.chemosphere.2013.09.016.

Shah, A. N., Tanveer, M., Shahzad, B., Yang, G., Fahad, S., Ali, S., Bukhari, M. A., Tung, S. A., Hafeez, A., & Souliyanonh, B. (2017). Soil compaction effects on soil health and cropproductivity: an overview. *Environmental Science and Pollution Research*, *24*(11), 10056-10067. https://doi.org/10.1007/s11356-017-8421-y.

Shao, W., Ni, J., Leung, A. K., Su, Y., & Ng, C. W. W. (2017). Analysis of plant root–induced preferential flow and pore-water pressure variation by a dual-permeability model. *Canadian Geotechnical Journal*, *54*(11), 1537-1552. https://doi.org/10.1139/cgj-2016-0629.

Šimůnek, J., Šejna, M., Saito, H., Sakai, M., & van Genuchten, M. T. (2009). The HYDRUS software package for simulating two-and three-dimensional movement of water, heat, and multiple solutes in variably-saturated media (Vol. 1). Department of Environmental Sciences, University of California, Riverside. https://www.pc-progress.com/Downloads/Pgm_hydrus1D/HYDRUS1D-4.08.pdf

Šimůnek, J., van Genuchten, M. T., & Šejna, M. (2008). Development and Applications of the HYDRUS and STANMOD Software Packages and Related Codes. *Vadose Zone Journal*, *7*(2), 587-600. https://doi.org/10.2136/vzj2007.0077.

Singh, K., Mishra, A. K., Singh, B., Singh, R. P., & Patra, D. D. (2016). Tillage Effects on Crop Yield and Physicochemical Properties of Sodic Soils. *Land Degradation & Development*, *27*(2), 223-230. https://doi.org/10.1002/ldr.2266.

Tang, X. Y., Katou, H., & Suzuki, K. (2020). Liming effects on dissolved and colloid-associated transport of cadmium in soil under intermittent simulated rainfall. *Journal of Hazardous Materials*, *400*, 123244. https://doi.org/10.1016/j.jhazmat.2020.123244.

Toor, G. S., & Sims, J. T. (2015). Managing Phosphorus Leaching in Mid-Atlantic Soils: Importance of Legacy Sources. *Vadose Zone Journal*, *14*(12), vzj2015.2008.0108. https://doi.org/10.2136/vzj2015.08.0108.

de Moraes, M. T., Debiasi, H., Carlesso, R., Franchini, J. C., da Silva, V. R., & da Luz, F. B. (2016). Soil physical quality on tillage and cropping systems after two decades in the subtropical region of Brazil. *Soil and Tillage Research*, *155*, 351-362. https://doi.org/10.1016/j.still.2015.07.015.

van Genuchten, M. T. (1980). A Closed-form Equation for Predicting the Hydraulic Conductivity of Unsaturated Soils. *Soil Science Society of America Journal*, *44*(5), 892-898. https://doi.org/10.2136/sssaj1980.03615995004400050002x.

van Genuchten, M. T., Leij, F., & Yates, S. (1991). The RETC code for quantifying the hydraulic functions of unsaturated soils. https://cfpub.epa.gov/si/si_public_record_Report.cfm?Lab=NRMRL&dirEntryId=130162.

Vereecken, H., Schnepf, A., Hopmans, J. W., Javaux, M., Or, D., Roose, T., Vanderborght, J., Young, M. H., Amelung, W., Aitkenhead, M., Allison, S. D., Assouline, S., Baveye, P., Berli, M., Brüggemann, N., Finke, P., Flury, M., Gaiser, T., Govers, G., Ghezzehei, T., Hallett, P., Franssen, H. J. H., Heppell, J., Horn, R., Huisman, J. A., Jacques, D., Jonard, F., Kollet, S., Lafolie, F., Lamorski, K., Leitner, D., McBratney, A., Minasny, B., Montzka, C., Nowak, W., Pachepsky, Y., Padarian, J., Romano, N., Roth, K., Rothfuss, Y., Rowe, E. C., Schwen, A., Šimůnek, J., Tiktak, A., Van Dam, J., van der Zee, S. E. A. T. M., Vogel, H. J., Vrugt, J. A., Wöhling, T., & Young, I. M. (2016). Modeling Soil Processes: Review, Key Challenges, and New Perspectives. *Vadose Zone Journal*, *15*(5), vzj2015.2009.0131. https://doi.org/10.2136/vzj2015.09.0131.

Wang, G., Fang, Q., Wu, B., Yang, H., & Xu, Z. (2015). Relationship between soil erodibility and modeled infiltration rate in different soils. *Journal of Hydrology*, *528*, 408-418. https://doi.org/10.1016/j.jhydrol.2015.06.044.

Watanabe, F. S., & Olsen, S. R. (1965). Test of an Ascorbic Acid Method for Determining Phosphorus in Water and NaHCO3 Extracts from Soil. *Soil Science Society of America Journal*, *29*(6), 677-678. https://doi.org/10.2136/sssaj1965.03615995002900060025x.

Wortmann, C. S., & Shapiro, C. A. (2008). The effects of manure application on soil aggregation. *Nutrient Cycling in Agroecosystems*, *80*(2), 173-180. https://doi.org/10.1007/s10705-007-9130-6.

Xu, B., Shao, D., Fang, L., Yang, X., Chen, S., & Gu, W. (2019). Modelling percolation and lateral seepage in a paddy field-bund landscape with a shallow groundwater table. *Agricultural Water Management*, *214*, 87-96. https://doi.org/10.1016/j.agwat.2018.11.008.

Yang, J., Nie, Y., Chen, H., Wang, S., & Wang, K. (2016a). Hydraulic properties of karst fractures filled with soils and regolith materials: Implication for their ecohydrological functions. *Geoderma*, *276*, 93-101. https://doi.org/10.1016/j.geoderma.2016.04.024.

Yang, Q., Luo, W., Jiang, Z., Li, W., & Yuan, D. (2016b). Improve the prediction of soil bulk density by cokriging with predicted soil water content as auxiliary variable. *Journal of Soils and Sediments*, *16*(1), 77-84. https://doi.org/10.1007/s11368-015-1193-4.

Yi, J., Qiu, W., Hu, W., Zhang, H., Liu, M., Zhang, D., Wu, T., Tian, P., & Jiang, Y. (2020). Effects of cultivation history in paddy rice on vertical water flows and related soil properties. *Soil and Tillage Research*, *200*, 104613. https://doi.org/10.1016/j.still.2020.104613.

Zhang, M. K. (2008). Effects of Soil Properties on Phosphorus Subsurface Migration in Sandy Soils. *Pedosphere*, *18*(5), 599-610. https://doi.org/10.1016/S1002-0160(08)60054-5.

Zhang, Z. B., Zhou, H., Lin, H., & Peng, X. (2016). Puddling intensity, sesquioxides, and soil organic carbon impacts on crack patterns of two paddy soils.

Geoderma, *262*, 155-164. https://doi.org/10.1016/j.geoderma.2015.08.030.

Zhang, Z. B., Zhou, H., Zhao, Q. G., Lin, H., & Peng, X. (2014). Characteristics of cracks in two paddy soils and their impacts on preferential flow. *Geoderma*, *228-229*, 114-121. https://doi.org/10.1016/j.geoderma.2013.07.026.